J Electroceram (2008) 21:238–241
DOI 10.1007/s10832-007-9142-2

Grain-size effects on the hardness of nanograin $BaTiO_3$ ceramics

X. Y. Deng · X. H. Wang · Z. L. Gui · L. T. Li · I. W. Chen

Published online: 17 May 2007

Abstract Dense nanocrystalline $BaTiO_3$ (BT) ceramics with grain size (GS) 50 nm were successfully prepared by spark plasma sintering (SPS) method. The nanoindentation experiment was used to test the hardness of different GS BT ceramics. It was found that the hardness of 50 nm nanograin BT ceramics increased 82% than that of 1.2 μm BT ceramics fabricated by conventional sintering (CS) process. Dislocation pinning resulting from the increase of grain boundary by ultrafine GS are believed to be the dominant factor in raising strength. Restriction on dislocation generation and mobility due to the domain wall motion and sliding imposed by ultrafine GS are expected to be exceptionally important. At the same time, the large stress in nanograin BT ceramics may also play a role in producing high strength. These differences of the hardness behavior between BT ceramics are attributed to the variation of the resultant microstructure, especially the GS of the ceramics.

Keywords Barium titanate · Grain size · Hardness · Spark plasma sintering

X. Y. Deng · X. H. Wang (✉) · Z. L. Gui · L. T. Li
State Key Lab of New Ceramics and Fine Processing,
Department of Materials Science and Engineering,
Tsinghua University,
Beijing 100084, People's Republic of China
e-mail: wxh@tsinghua.edu.cn

I. W. Chen
Department of Materials Science and Engineering,
University of Pennsylvania,
Philadelphia, PA 191046272, USA

1 Introduction

The perovskite structure BT has been extensively used in the electronic industry for its high dielectric constant, including the fabrication of multilayer ceramic capacitors, piezoelectric transducers and ferroelectric memories [1]. With the continuous advance in microelectronics and communications, electrical devices have been miniaturized and used under quite severe atmospheres. For examples, a stress of 30–50 MPa is generated in the capacitor during end termination and soldering. In multilayer piezoelectric actuators, the high electric driving field needed to produce a large displacement may cause mechanical and electrical degradation [2]. Therefore BT-based ceramics with high mechanical properties and reliabilities are strongly required as well as stable dielectric properties.

Nanocrystalline materials form an exciting area of materials research because bulk materials with GS less than 100 nm have some properties not seen in their microcrystalline counterparts [3]. In the past years, a variety of theoretical and experimental studies [4, 5] had been made about the nanocrystalline BT ceramics focusing on the size dependence of polarization, Curie temperature (T_C) and tetragonal distortion (c/a-1, where c and a are the unit cell edges), such as the theoretical models based on the Landau–Ginsburg–Devonshire (LGD) theory in the case of isolated particles [6]. However, the research of mechanical properties of BT ceramics is scanty, especially in dense nanograin samples, which depends strongly on the microstructure.

In this paper, dense nanocrystalline BT ceramics with GS 50 nm were successfully compacted to full density by SPS. We discussed the GS effects on the hardness of nanograin BT ceramics compared with the coarse-grained specimens.

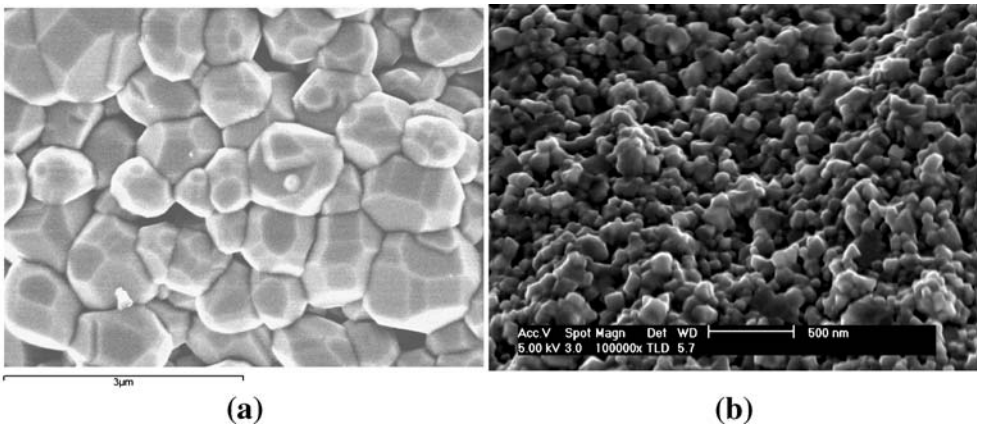

Fig. 1 (**a**) SEM image of the BT ceramics sintered at 1200 °C by CS. (**b**) SEM image of the BT ceramic sintered at 850 °C by SPS

2 Experiment

Ultrafine pure BT powders were obtained by a modified oxalate precipitation method as described previously [7]. The particle size was nearly spherical from 20 to 30 nm. The main impurities contained in the powders were at the following levels: 0.04 wt.% Sr, 0.02 wt.% Na, and 0.006 wt.% K. High-purity 50 nm BT ceramics was prepared by SPS, which is a pressure assisted fast sintering method based on high-temperature spark plasma momentarily generated in the gaps between powder materials by electrical discharge during on–off direct current (d.c.) pulse. It has been suggested that the d.c. pulse could generate several effects: spark plasma, spark impact pressure, Joule heating and an electrical field diffusion effect [8]. Through these effects, SPS can rapidly consolidate powders to near-theoretical density through the combined effects of rapid heating rate and pressure.

The samples were heated up at 400 °C/min with an uniaxial pressure of 70 MPa and sintered at 850 °C for 2 min. The samples were then annealed in air for 10 h at 600 °C. This treatment could guarantee the relief of residual stresses and the elimination of excess oxygen vacancies possibly produced during SPS. Final SPS specimen size is a 20 mm diameter disk with a thickness of 2–4 mm. For the CS, the same BT nano-powder were pressed into pellets and subsequently sintered in air for 2 h at 1200 °C.

The bulk density was determined by using the Archimedes method. The X-ray diffraction (XRD) data were collected using Cu-Kα radiation. The microstructural evolution during sintering was investigated by scanning electron microscopy (SEM), which was performed on SEM-450 and FP6800/73. GS was calculated from the broadenness of the (111) peak of XRD and estimated from SEM images with additional characterization by analytical electron microscopy. The hardness of the nanograin BT ceramics was characterized with a MTS nanoindenter XP (MTS Systems Corporation, Oak Ridge, TN) equipped with a diamond Berkovich indenter with a reported tip radius of less than 50 nm. Experiments were performed in a clean-air environment of ~45% relative humidity and 22 °C ambient temperature.

3 Results and discussion

Figure 1 shows SEM image of BT ceramics by CS at 1200 °C and by SPS at 850 °C, respectively. Table 1 lists the processing conditions and the resultant properties of BT ceramics in this study. Average GS of BT ceramics sintered by SPS was approximately 50 nm, while that by CS was about 1.2 μm. Smaller GS can be obtained by SPS under lower temperature. Figure 2 shows the variation in hardness and load vs. contact depth using the continuous stiffness measurement (CSM) option, calculated from 10 indentations, covering the loading range 0.003–128 mN. The loading rate was 0.05 mN/s and the dwell time 50 s in all the tests. The hardness of 50 nm nanograin BT ceramics enhanced 82% than that of 1.2 μm BT ceramics fabricated by CS.

The effect of GS on the hardness of nanocrystalline materials has been reported to have the form shown schematically in Fig. 3 [9, 10]. The influence of GS on the hardness H at $d > dc$ (critical grain size) is here considered to represent the motion of dislocations and is given by the Hall–Petch equation:

$$H = H_i + kd^{-1/2} \tag{1}$$

Table 1 Processing conditions and the resultant properties of BT ceramics.

GS (nm)	Sintering condition	Sintering temperature (°C)	Relative density (%)	Hardness (GPa)
50	SPS	850	97	8.2
1200	CS	1200	95	4.5

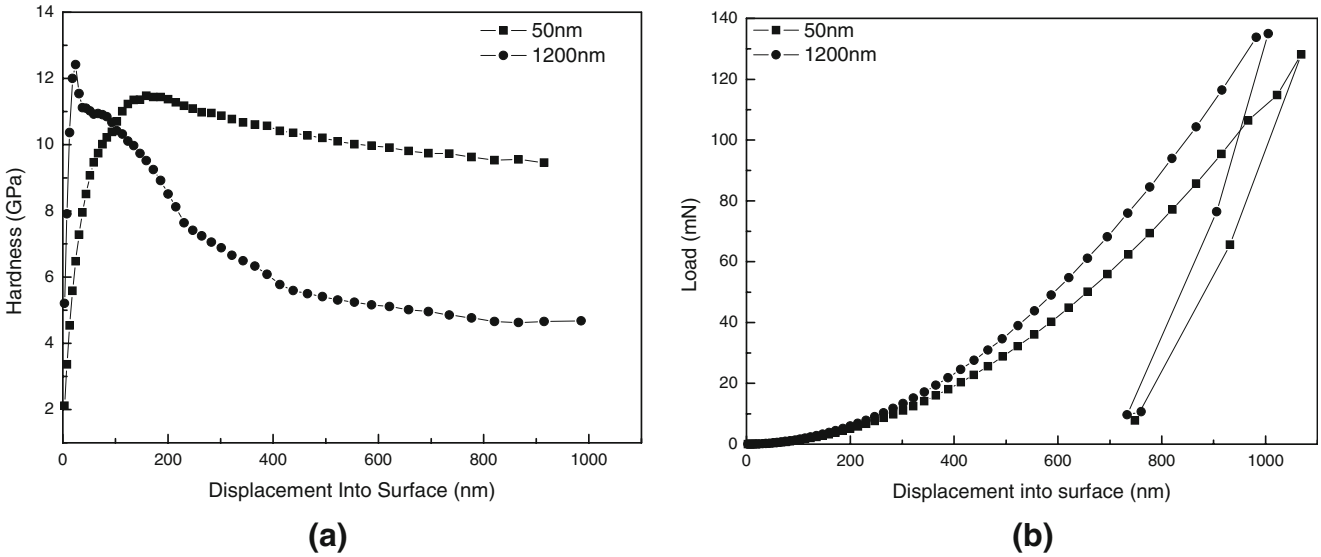

Fig. 2 Evolution of (**a**) the hardness and (**b**) load of different GS BT ceramics vs. indentation contact depth

Where H_i is the lattice friction stress and k is the Hall–Petch constant commonly interpreted to represent the stress needed to extend dislocation activity into grains adjacent to grains that have already yielded [11]. Dislocation mechanisms which can lead to this equation are given in the following three models: (a) the GS work hardening model by Conrad [12–14]; (b) the grain boundary ledge model by Li [15]; and (c) the geometric accommodation and statistically stored dislocation model by Ashby [16].

In present study, the 50 nm nanograin and 1.2 μm BT ceramics belong to this range ($d > dc$). The relationship between hardness and GS of BT ceramics is consistent with the Eq. 1.

Figures 4 and 5 show ferroelectric domain and grain boundary of 50 nm BT nanograin ceramics. With the decrease of GS, the relative volume of grain boundaries increase, dislocation pinning will occur, so dislocation pinning resulting from the increase of grain boundary are believed to be the dominant factor in raising strength [16, 17]. Also, with the decrease of GS, BT ceramics transform from tetragonal to cubic phase and induce ferroelectric relaxation, domain wall motion and sliding at the same time. Therefore, restriction on dislocation generation and mobility due to the domain wall motion and sliding imposed by ultrafine GS are expected to be exceptionally important [17]. Additionally, the large stress in nanograin BT ceramics [18] may also play a role in producing high strength. It is believed that one relaxation process exists in all the ferroelectric phase, which demonstrates a memory effect of ferroelectric domain configuration [19], in the mean time local compressional and tensile stresses will take place.

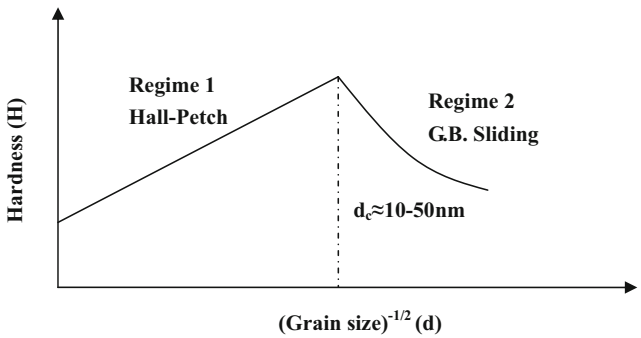

Fig. 3 Schematic profile of the variation of hardness (H) with grain size (d)

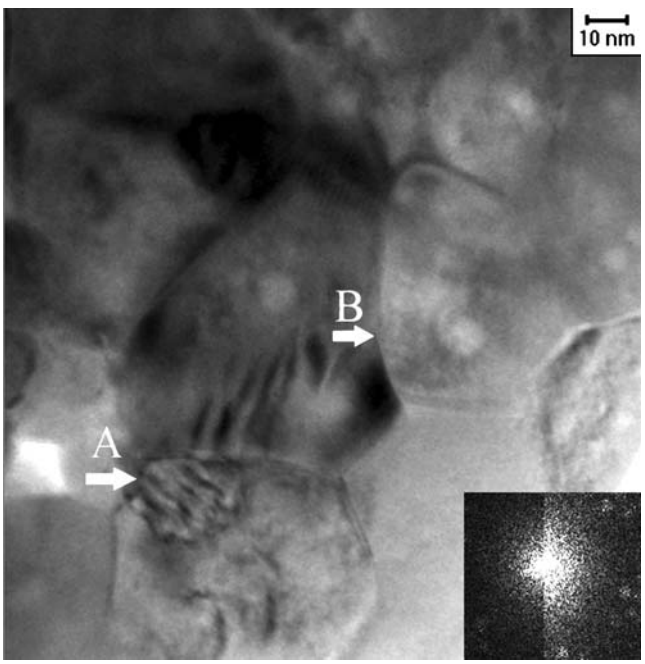

Fig. 4 Ferroelectric domain (A) and grain boundary (B) of 50 nm BT ceramics

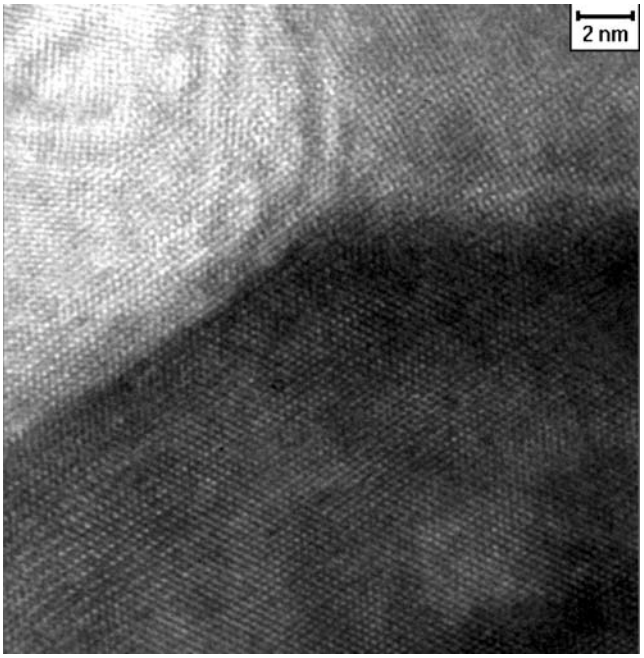

Fig. 5 Grain boundary of 50 nm BT ceramics

4 Conclusion

Dense nanocrystalline BT ceramics with GS 50 nm were successfully prepared by SPS. The nano indentation experiment revealed that the hardness of 50 nm nanograin BT ceramics increased 82% than that of 1.2 μm BT ceramics fabricated by CS. Dislocation pinning resulting from the increase of grain boundary by ultrafine GS are believed to be the dominant factor in raising strength. Restriction on dislocation generation and mobility due to the domain wall motion and sliding imposed by ultrafine GS are expected to be exceptionally important. Furthermore, the large stress in nanograin BT ceramics may also play a role in producing high strength.

Acknowledgement This work was supported by the High Technology Research and Development Project, China under Grant No. 863-2001AA325010, and the Ministry of Science Technology, China through 973-project under Grant No. 2002CB613301, and also supported by National Center for Nanoscience and Technology, China.

References

1. H.J. Hwang, K. Niihara, J. Mater. Sci. **33**, 549 (1998)
2. W.H. Tuan, S.K. Lin, Ceram. Int. **25**, 35 (1999)
3. G.D. Zhan, J.D. Kuntz, J.L. Wan, A.K. Mukherjee, Nature Mater. **2**, Jan (2003)
4. G. Arlt, D. Hennings, G. De, J. Appl. Phys. **58**(4), 15 (1985)
5. M.H. Frey, D.A. Payne, Phys. Rev. **B 54**(5), 3158 (1996)
6. Z. Zhao, V. Buscaglia, M. Viviani, M.T. Buscaglia, L. Mitoseriu, A. Testino, M. Nygren, M. Johnsson, P. Nanni, Phys. Rev. **B 70**, 024107-1 (2004)
7. X.H. Wang, R.Z. Chen, L.T. Li, Z.L. Gui, Ferroelectrics **262**(1–4), 1225 (2001)
8. M. Omori, Mater. Sci. Eng. **A 287**, 183 (2000)
9. S. Rattanachan, Y. Miyashita, Y. Mutoh, J. Eur. Ceram. Soc. **23**, 1269 (2003)
10. P.H. Xiang, X.L. Dong, C.D. Feng, H. Chen, Y.L. Wang, Mater. Res. Bull. **38**, 1147 (2003)
11. H. Conrad, J. Narayan, Scr. Mater. **42**, 1025 (2000)
12. H. Conrad, G. Thomas, J. Wasburn, Interscience (New York, 1961), p. 299
13. H. Conrad, Acta Metall. **11**, 75 (1963)
14. H. Conrad, J. Burke, V. Weiss, *Ultrafine-grain metals* (Syracuse University Press, Syracuse, NY, 1970), p. 213
15. C.M. Li, Trans. Tms–Aime. **227**, 239 (1963)
16. M.F. Ashby, Phil. Mag. **21**, 399 (1970)
17. K. Lu, Mater. Sci. Eng. **R16**, 161 (1996)
18. W.R. Buessem, L.E. Cross, A.K. Goswami, J. Am. Ceram. Soc. **49**(1), 33 (1966)
19. B.L. Cheng, B. Su, J.E. Holmes, T.W. Button, M. Gabbay, G. Fantozzi, J. Electroceram. **9**, 17 (2002)